JOURNAL OF MATERIALS SCIENCE 8 (1973) 1373–1382

Steel disc reinforced polycarbonate

B. GLAVINCHEVSKI, M. PIGGOTT
Department of Chemical Engineering, Materials Research Centre, University of Toronto, Canada

Stainless steel platelets have been embedded in polycarbonate under carefully controlled conditions, so that the strength of the components and the interface were known with confidence. It was observed that the strength of the composite depended on the volume fraction of platelets according to a modified rule of mixtures expression. No dependence on aspect ratio of the platelets was observed for aspect ratios in the range 100 to 800, and round and square platelets gave substantially the same results. Although strength improvement is biaxial in the case of platelets (while it is uniaxial for aligned fibres) the gain in strength along one direction is at the expense of strength along the other.

1. Introduction

The use of planar reinforcement is considered to have considerable advantage over fibre reinforcement since the potential strengthening and stiffening effects are inherently two dimensional rather than one dimensional. Early investigation of the use of glass met with disappointment owing, at least in part, to the difficulty of making discs with adequate strength [1]. Little success was obtained with silicon carbide either, although the platelets were strong [2]. It seems likely that the main problems were brittleness, and lack of control of the interface. More success has been achieved with aluminium boride [3], and moderate success has been achieved with mica [4], which has the virtue of being a very cheap material.

In the early work mentioned, there was considerable discussion of the theory, and more recently Padawer and Beecher [5] have adapted elasticity treatments of fibre reinforcement to the case of planar reinforcement. However, the field appears to lack data against which the theories may be tested, and the interface failure problems most workers seem to have encountered preclude the application of elasticity theory.

When interface failure takes place the plasticity theories used for reinforced metals appear to be appropriate [6]. In view of this, for this study a matrix material was chosen which has flow properties similar to soft metal. Efforts were made to ensure that matrix shear flow occurred at the platelet matrix interface, so that the interfacial shear force was known.

2. Experimental method and results

Stainless steel platelets were used, so that the reinforcement had well-defined, reproducible, properties. Tensile tests on strips of the steel (type 302 stainless) indicated that the strength depended to some extent on steel thickness (Table I), but was reproducible to within less than 1%.

TABLE I Tensile strength of stainless steel.

Thickness (mm)	Strength GN m^{-2}
0.025	1.8
0.05	1.5
0.10	1.6
0.20	1.8

Polycarbonate was employed as matrix, since it is ductile, has a well-defined flow stress, and exhibits considerable plastic flow with little change in stress. General Electric Lexan bisphenol-A polycarbonate 140-111 was used.

Considerable effort was made to obtain a reproducible interface between steel and polycarbonate. After much preliminary study it was found that good results were obtained if the steel was first degreased in trichlorethylene, then immersed for 40 min at 70 to 80° C in a solution of sodium hydroxide (1.1 wt %) together with sodium pyrophosphate (2.2%), metasilicate (1.1%) and alkyl-lauryl sulphate (0.36%), then

etched in hot concentrated sulphuric acid containing some sodium dichromate (1.7%), and finally immersed in hot 2.5 M caustic soda, washed, carefully dried, and kept dry in a desiccator.

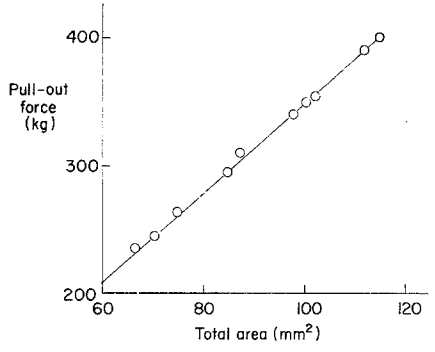

Figure 1 Results of pull-out tests.

A very thin adhesive layer of epoxy resin (Shell Epon 828) was applied to the clean steel from a dilute solution in chloroform. Strips of steel prepared in this manner were partly embedded in polycarbonate, and pull-out tests were carried out. Fig. 1 shows the results obtained. It can be seen that the pull-out force varied linearly with total contact area. The slope of the line gives a value for the critical shear stress of 35 MN m^{-2}, indicating that the interfacial region has the same shear strength as the polycarbonate matrix. The closeness of the points to the line shows that good reproducibility of the bond was achieved, and the polycarbonate surface close to the strip end dimpled when pull-out took place, confirming that plastic flow occurred in the polycarbonate when the strip pulled out.

Composites were made by cutting square pieces of steel strip, and placing them carefully on a strip of polycarbonate at the bottom of a suitably shaped mould. Another sheet of polycarbonate was placed on top, then another layer of steel was placed on top of this and arranged so that the gaps in the steel layer were above the centres of the steel squares in the first layer. This was followed by another layer of polycarbonate, then a layer of steel squares with the centres over the gaps in the second layer. Finally a layer of polycarbonate was placed on top, and the whole assembly was moulded at 200° C for 2 h under slight pressure to prevent shrinkage of the polymer.

Cooling was carried out under increasing pressure, reaching 7 MN m^{-2} at 175° C, and pressure was released when the temperature had fallen to 130° C.

Fig. 2 shows typical specimens, one with square plates, as above, and one with circular discs, made in the same way. Some specimens were made with four or more layers of steel. The steel squares were all 20 mm along one side, and the circular discs were 20 mm diameter. The aspect ratio was varied by varying the thickness of the steel. To keep volume fraction roughly constant the thickness of the polycarbonate sheet was varied.

The specimens were tested in an Instron machine at a speed of 0.1 cm min^{-1}. One or two did not fail in the gauge length, and have been excluded from the results.

It was found that strength was independent of aspect ratio. Fig. 3 shows a plot of α against aspect ratio. α is the reinforcement efficiency factor, used in the empirical relationship,

$$\sigma_{cu} = \alpha V_p \sigma_{pu} + (1 - V_p) \sigma_{mu}$$

where V_p = volume fraction of platelets, and the σ's are ultimate tensile strengths for composite (σ_{cu}), platelets, (σ_{pu}) and matrix (σ_{mu}).It may be seen that α does not show any significant variation, and is substantially the same for round plates and square plates. Each point on the curve is the average from at least two specimens, and the agreement between specimens was better than $\pm$ 2%.

The strength varied linearly with volume fraction. Fig. 4 is a plot of results from specimens with all aspect ratios, and the results are close to a line which extrapolates to intersect the stress axis at the strength of the polycarbonate.

Fig. 5 shows a typical Instron record obtained with a reinforced specimen. The strain values are calculated by assuming that the early part of the stress-strain curve obeys the rule of mixtures. For comparison, the curve obtained for the steel strip is included with the ordinate adjusted to 30% of the true value. The unreinforced polycarbonate broke at a strain of more than 100%, and typically withstood a maximum nominal stress of 65 MN m^{-2}.

3. Discussion

Since the pull-out tests show that the polycarbonate shears when the steel strip is pulled out, and since polycarbonate flows with little increase

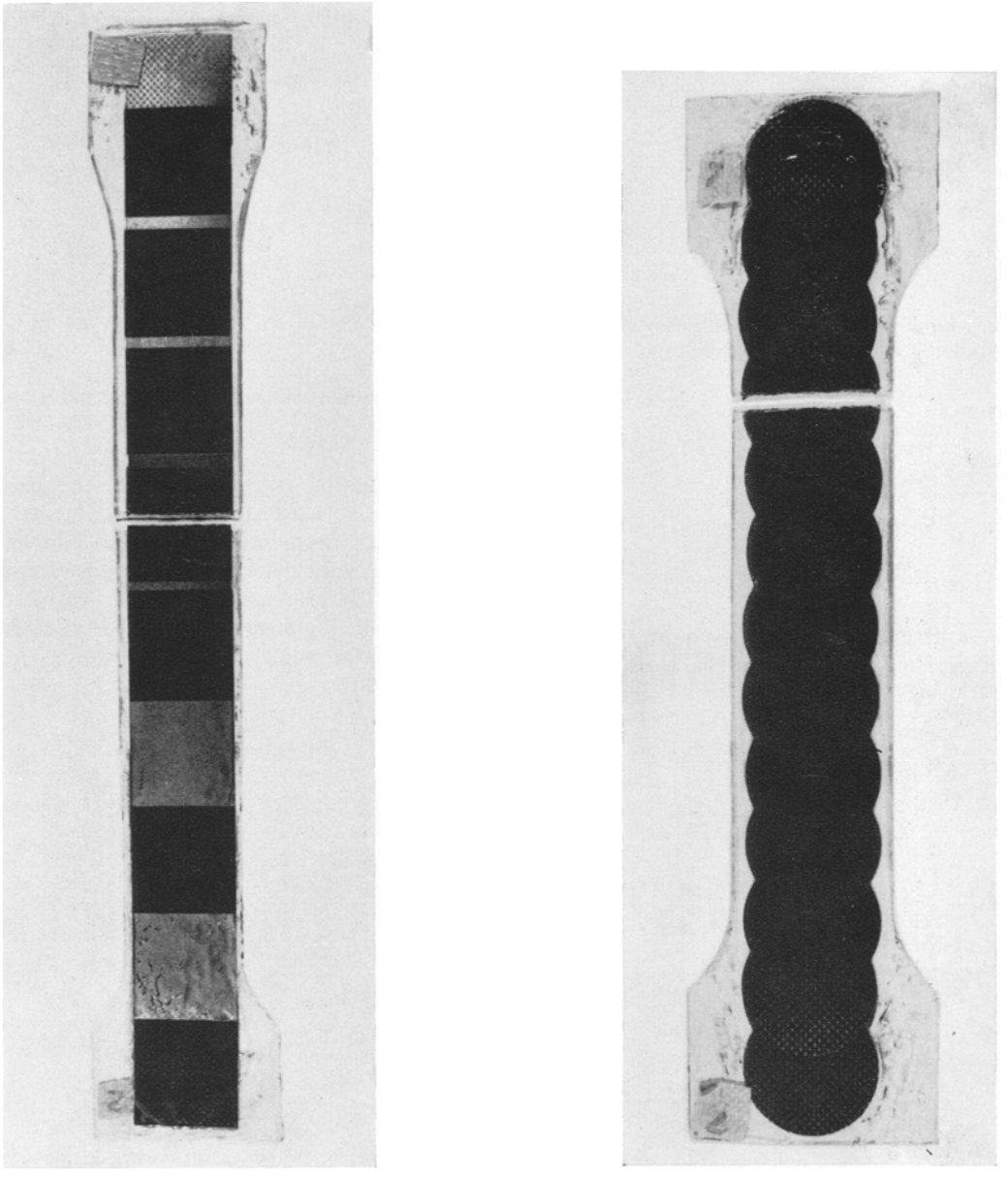

Figure 2 Specimens of steel reinforced polycarbonate after testing to failure in tension.

in stress after the yield point, the reinforcement theory for fibres in ductile metals [7] is applicable to the composites described here. The only difference between the fibre and platelet case should be a numerical factor to allow for the different geometry, and the effects of stress transfer from one plane of platelets, to adjacent planes, at the platelet boundaries normal to the stress. The effects are similar to those at fibre ends indicated by Piggott [6] and examined in detail by Riley [8].

The rate of increase of stress with distance, x from the end of a platelet will be

$$\frac{d\sigma_p}{dx} = \frac{2\tau_y}{t}$$

where τ_y is the matrix shear flow stress, and t

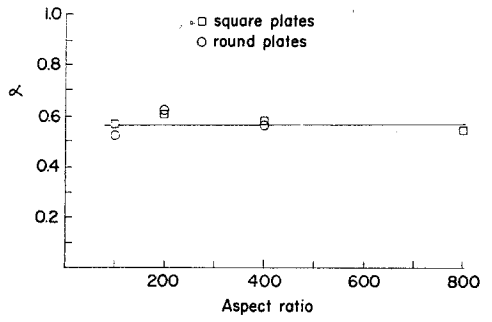

Figure 3 Empirical parameter for efficiency of strengthening, α, plotted as a function of aspect ratio.

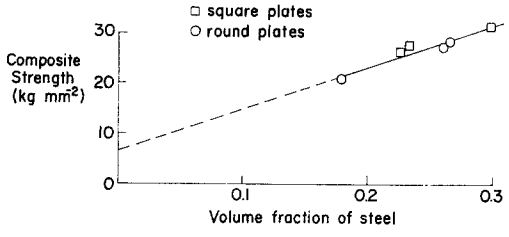

Figure 4 Relation between volume fraction of platelets and tensile strength of composite. Specimens have aspect ratios varying from 100 to 800.

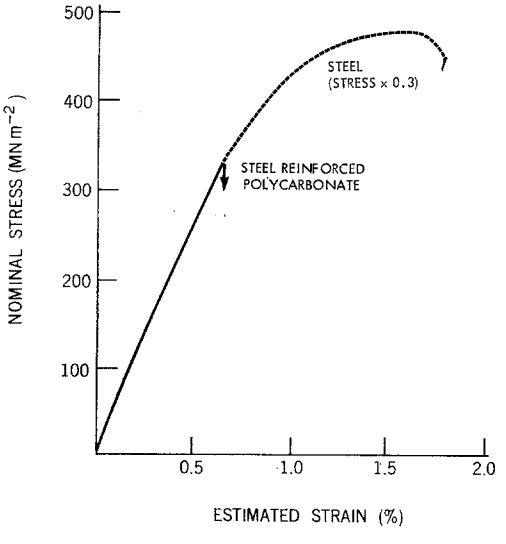

Figure 5 Stress strain curves for steel, and composite with $V_t = 0.3$ mm platelets with an aspect ratio of 200.

is the platelet thickness. The critical length for pull-out, $2l_c$ is then

$$2l_c = \frac{\sigma_{pu}\, t}{\tau_y} = 47t$$

for the steel and polycarbonate used here.

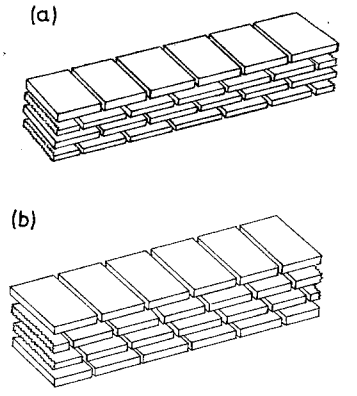

Figure 6 Two possible packing arrangements for square platelets.

The situation for a platelet in the packing arrangement used in the experiments (for packing arrangements see Fig. 6a) and having twice this critical aspect ratio (corresponding to $2L/t \simeq 100$) is shown in Fig. 7a. At the centre of the plate the stress is twice the average, to allow for the adjacent platelet endings at the platelet centre.

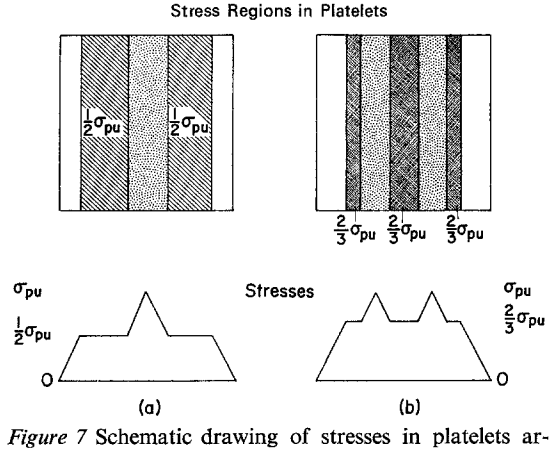

Figure 7 Schematic drawing of stresses in platelets arranged as shown in Fig. 6(a) and (b) for an aspect ratio of about twice the critical value. The upper drawings are platelets viewed from above, and the regions with different stress regimes are distinguished by the shading.

It is clear from this drawing why no aspect ratio effect is observed with square platelets packed this way; the area of the triangle at the centre is just sufficient to make the average stress exactly $\frac{1}{2}\,\sigma_{pu}$. This applies for all aspect ratios greater than the critical value of 47, and the strength of the composite in this range can thus be expressed by the equation:

$$\sigma_{cu} = \tfrac{1}{2}\sigma_{pu} V_p + (1 - V_p)\sigma_{mu} .$$

However, if the platelets in adjacent layers are arranged differently, a slight aspect ratio effect should be obtained. Fig. 7b shows the effect of staggering the gaps in adjacent layers. The composite strength is then

$$\sigma_{cu} = \tfrac{2}{3}\sigma_{pu} V_p \left(1 - \frac{l_c}{6L}\right) + (1 - V_p)\sigma_{mu}$$

for all aspect ratios greater than 1.33 times the critical. This is discussed more fully in the Appendix where this expression is derived. The aspect ratio effect is much smaller than with fibres, since the range of variation of α is only from 0.50 to 0.67, instead of 0.5 to 1.0 and the $(1 - (l_c/6L))$ term tends to the value 1 three times as quickly as with fibres.

In the case of the circular discs there should be a slight aspect ratio effect. If the platelets in adjacent layers are symmetrically arranged in rows as shown in Fig. 8a (this was the arrangement used for the experiments) the stresses in the platelets will have a complicated pattern (Fig. 8b) because at the centre of a platelet, other platelets in adjacent layers will be shedding their loads. This is discussed fully in the Appendix; Fig. 9 indicates the expected variation of α with aspect ratio. Also included are curves for the two square platelet cases already discussed.

In addition, Fig. 9 has a curve for platelets arranged in adjacent layers in the close packed hexagonal arrangement (as in crystals of zinc, for example). The platelet stresses resulting from load transfer by matrix shear are shown schematically in Fig. 10, the complex pattern in the centre again being due to platelets in adjacent layers shedding their loads, and again this case is discussed in the Appendix.

For the arrangement used in the experiments, the observation that α is close to 0.5 can thus be accounted for theoretically. It seems likely that other efficient packing arrangements will give similar results, since the hexagonal arrangement differs very little from the linear arrangement.

In all cases, as the specimens failed, platelets failed by fracture across their diameters (or across their centre in the case of square platelets); thus the platelets break where the theory indicates that the stresses should be greatest.

Although the linear increase of strength with volume fraction (Fig. 4) suggests that quite high strengths can be obtained (at least 700 MN m^{-2} at $V_p = 0.78$), there seems to be almost no advantage in using platelets over fibres from the point of view of maximizing strength in sheets

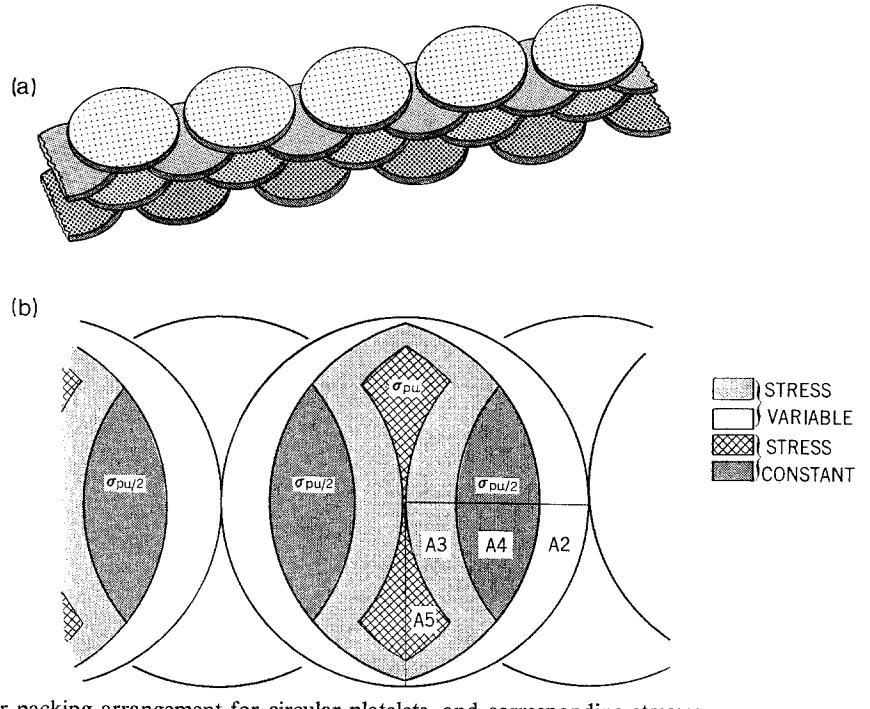

Figure 8 Linear packing arrangement for circular platelets, and corresponding stresses.

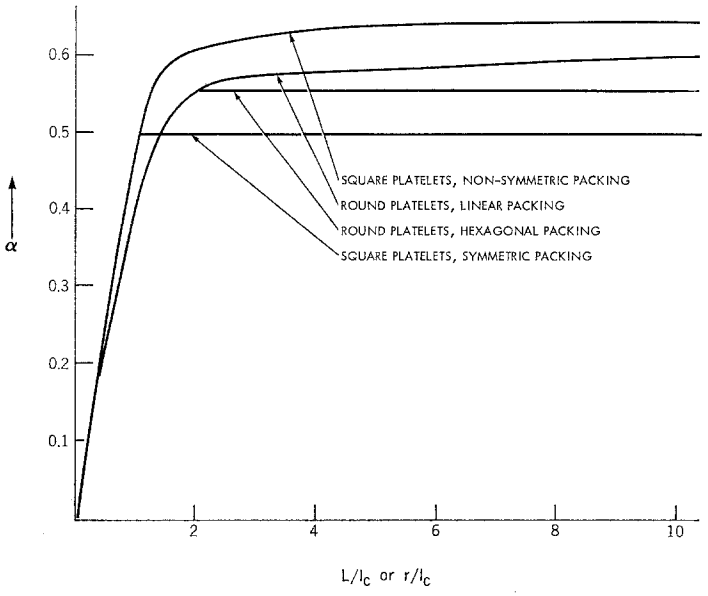

Figure 9 Theoretical prediction for strengthening efficiency factor, α, as a function of aspect ratio.

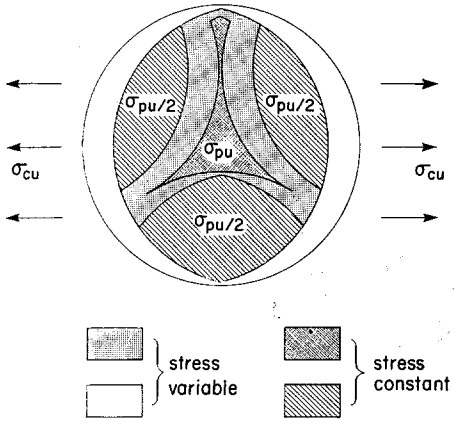

Figure 10 Schematic drawing of stresses in hexagonally packed circular platelets.

of material. Although the strength is biaxial with platelets, the value of α is $\frac{1}{2}$. With fibres the strength is uniaxial but α can approach 1, so that substantially biaxial strength can be obtained by using fibres in layers at right angles to each other, when α would fall to $\frac{1}{2}$, the same as for platelets. The possible higher volume fractions that might be achieved with platelets is offset by the greater risk of seriously weakening defects in laminar materials.

From the point of view of biaxial stiffness, however, there should be an advantage in using platelets. For toughness also, platelets have advantages. Toughness is generally greatest for fibres and platelets having the critical aspect ratio [9], so there is no trade-off between toughness and strength for platelet reinforcement, as there is for fibre reinforcement. In addition, platelets would give biaxial toughening, whereas fibre reinforced materials risk being brittle for stresses oblique to the fibres [10]. The material described here should have a potential fracture surface energy of 100 kJ m^{-2} from pull-out effects alone. In addition, both components can deform plastically to a considerable extent. However, the stress-strain curve does not deviate significantly from a straight line, and failure appears to occur at strains below the yield strain of the steel. This is probably because of the stress concentrations in the steel resulting from adjacent platelets unloading their stresses.

The results described here are in reasonably good agreement with those of Woodhams *et al* [4] on mica. From their plot of strength versus aspect ratio, it can be seen that above an aspect ratio of about 130 there is little change of strength with aspect ratio. Below 130 there is a rapid falling-off in strength, indicating that pull-out is taking place. The strength achieved suggests that their mica strength was about 850 MN m^{-2}, and the shear force at the interface was about 7.8 MN m^{-2}. This is very much less than the maximum shear force the resin could exert, which was about 28 MN m^{-2}.

4. Conclusion

There is very little to be gained by using platelets having aspect ratios greater than the critical for reinforcement. Round platelets give similar results to square ones, and steel reinforced polycarbonate can be made with a strength of about 300 MN m^{-2}, with the potential of increasing this to 700 MN m^{-2} by increasing the volume fraction.

Although the strength is biaxial, there is very little advantage in using platelets as compared with fibres so far as strength is concerned.

Acknowledgements

The research for this paper was supported by the Defence Board of Canada, grant number 7501-10. The authors are also indebted to Dr F. W. Maine and Dr P. D. Shepherd and others at Fiberglas Canada Limited for many useful discussions, and similarly to Dr R. T. Woodhams.

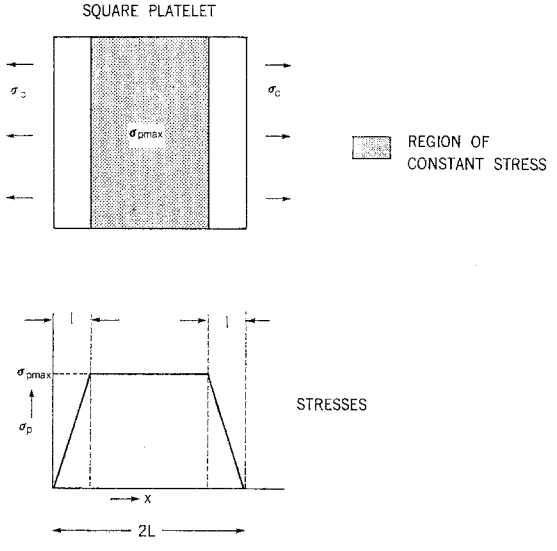

Figure 11 Stresses in a single embedded square platelet.

Appendix

Stresses in platelets embedded in a stressed perfectly plastic medium.

1. Square platelets

1.1. No adjacent platelets

The treatment is basically the same as that used by Kelly [7], for fibres. Equilibrium of surface and internal forces on the platelets causes the platelet stress to increase linearly from the end, Fig. 11, according to the equation

$$\frac{d\sigma_p}{dx} = \frac{2\tau_y}{t}$$

where t is the plate thickness, x is the distance from the end of the platelet, σ_p is the stress in the platelet, and τ_y is the flow stress of the matrix.

In the region near the centre of the platelet, the strains in matrix and platelet are equal, and the platelet stress is constant, having the value

$$\sigma_{pmax} = \frac{2\tau_y l}{t} \tag{1}$$

where l is the stress transfer length (Fig. 11).

The average platelet stress is, therefore,

$$\bar{\sigma}_p = \left\{\int_0^l \frac{2\tau_y x}{t}\,dx + \frac{2\tau_y l}{t}(L - l)\right\} \Big/ L$$

where the platelet length is $2L$,

$$\therefore \bar{\sigma}_p = \frac{2\tau_y l}{t}[1 - (l/2L)] \cdot \tag{2}$$

If a stress large enough to break the plate is applied, Equation 1 gives the critical plate length, $2l_c$, i.e.

$$2l_c = \frac{\sigma_{pu}}{\tau_y} t \tag{3}$$

and the average platelet stress becomes

$$\bar{\sigma}_p = \sigma_{pu}\left(1 - \frac{l_c}{2L}\right) \tag{4}$$

Thus, if the behaviour of the composite is expressed by the modified rule of mixtures expression

$$\sigma_{cu} = \alpha V_p \sigma_{pu} + (1 - V_p)\sigma_{mu}$$

then α will have the value

$$\alpha = 1 - \frac{\sigma_{pu} t}{4\tau_y L} \tag{5}$$

or, using Equation 3,

$$\alpha = 1 - l_c/2L \ . \tag{6}$$

For platelets with less than the critical aspect ratio, pull-out will occur, and the average platelet stress will be

$$\bar{\sigma}_p = \frac{\tau_y L}{t} = \sigma_{pu} L/2l_c \tag{7}$$

so that in this case

$$\alpha = L/2l_c \ . \tag{8}$$

1.2. Effect of adjacent plates

The treatment here follows that originally used by Riley [8] for fibre reinforced metals. Platelets having a symmetrical packing arrangement like

that shown in Fig. 6a will have stresses shown diagrammatically in Fig. 7a. The extra stress in the centre is the result of adjacent platelets unloading their stresses, and the linear increase is governed by the flow stress of the matrix, in the same way as for the stress increase at the platelet end.

Since the sloping parts of the graph representing the platelet stress all have the same slope, $d\sigma_p/dx = 2\tau_y/t$, the average stress in the platelet is

$$\bar{\sigma}_p = \sigma_{pmax}/2 \ . \qquad (9)$$

Consequently, failure of the composite will occur when the average platelet stress is $\sigma_{pu}/2$, no matter what the aspect ratio is, so long as it is greater than the critical value. Thus $\alpha = \frac{1}{2}$ for all aspect ratios above the critical.

In non-symmetrical packing arrangements, some small aspect ratio effect can be expected. Fig. 6b shows an arrangement not having a plane of symmetry, but where adjacent platelets end systematically at intervals of one third of the platelet length. Fig. 7b shows the corresponding platelet stresses, assuming that stress transfer can only take place at the rate $d\sigma_p/dx = 2\tau_y/t$. (Note that this implies that the matrix stress is not constant.)

So long as the platelet length exceeds $4l_c/3$, some plateau exists between the stress peaks as shown in the diagram, since the longer sloping parts occupy a length of plate $2l_c/3$, and the shorter parts occupy a length $l_c/3$. Thus when the stress peaks reach the U.T.S. the average platelet stress is

$$\bar{\sigma}_p = \tfrac{2}{3}\,\sigma_{pu}(1 - l_c/6L) \qquad (10)$$

(The average stress in platelets having lengths between l_c and $3l_c/4$ will not obey this relation exactly. A nearer approximation in this range is

$$\bar{\sigma}_p = \sigma_{pu}\left(\frac{5}{6} - \frac{l_c}{3L}\right),$$

making the assumptions that stress increases (or decreases) in platelets only at the aforementioned rate.)

For platelets having greater than the critical length the value of α is thus approximately

$$\alpha = 2(1 - l_c/6L)/3 \ . \qquad (11)$$

2. Round platelets

2.1. No adjacent platelets

This treatment is an extension of that used for square platelets. However, it must of necessity be more approximate because an additional assumption is required. Since the boundaries of the plates are curved, the lines of constant stress must also be curved. This curvature could either be neglected, giving the situation shown in Fig. 12, or assumed to be equal to the curvature of the plate edge, Fig. 13. Neglecting the curvature yields unlikely stress values at high aspect ratios, however. These arise because the lines of maximum constant stress, UV and WX are very close to the ends of the diameter, AF for high aspect ratio. Consequently, the stress along diameter YZ would have to be very much less than this.

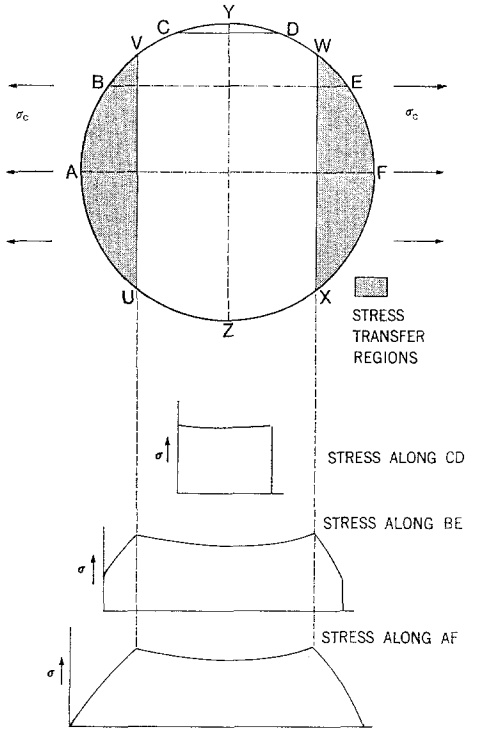

Figure 12 Stresses in a single embedded round platelet assuming isobars are normal to applied stress.

In this treatment the curvature will be assumed to be equal to the curvature of the edge of the plate. (An analysis of the straight lines of constant stress shows that for low aspect ratio, the results are very similar to the curved case [11].

The platelet may be regarded as divided into thin strips in the applied stress direction. Interaction between the strips is neglected, so that each strip will be subject to stress distributions similar to that for the square platelet; there will be a region at the ends where the stress increases linearly with distance from the end of the strip,

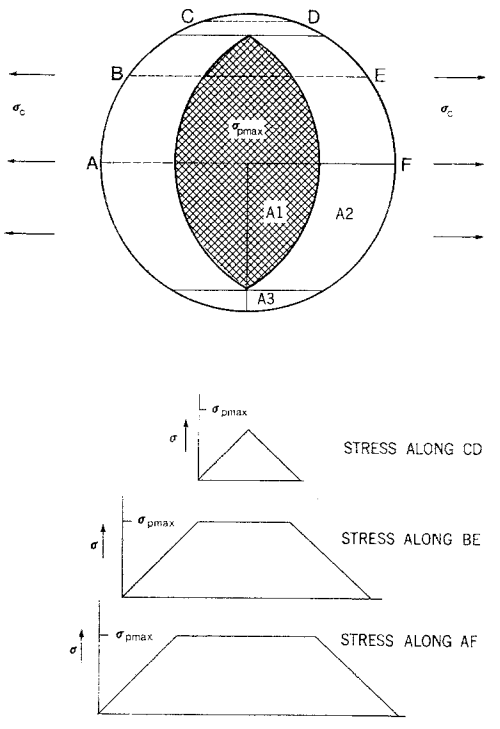

Figure 13 Stresses in a single embedded round platelet assuming isobars are parallel to platelet edge.

and for strips that are long enough, there will be a region where the stress is constant. Considering a quadrant of the platelet, the average stress, therefore, will be

$$\bar{\sigma}_p = \frac{4}{\pi r^2}(A_1 \sigma_{pmax} + \tfrac{1}{2} A_2 \sigma_{pmax} + A_3 \bar{\sigma}_3) \quad (12)$$

where A_1 is the area of region 1 (Fig. 13) where the stress is constant, A_2 is the area of region 2 where the stress increases linearly with distance from the edge up to the value σ_{pmax}, and A_3 and $\bar{\sigma}_3$ are respectively the area and average stress in region 3 where the stress never reaches σ_{pmax}.

Now

$$A_2 = l_c \sqrt{(r^2 - l_c^2)}$$

and

$$A_3 = \tfrac{1}{2}\left\{r^2\left(\frac{\pi}{2} - \sin^{-1}\sqrt{[1 - (l_c/r)^2]}\right) - l_c\sqrt{(r^2 - l_c^2)}\right\}$$

while

$$A_1 = \frac{\pi a^2}{4} - (A_2 + A_3) .$$

Now

$$A_3 \bar{\sigma}_3 = \frac{\tau_y}{t}\int_{\sqrt{(r^2 - t^2 c)}}^{r} (r^2 - x^2)\,dx$$

$$= \frac{\tau_y}{3t}[r - \sqrt{(r^2 - l_c^2)}]^2 [2r + \sqrt{(r^2 - l_c^2)}]$$

$$= \frac{\tau_y}{3t}[2r^3 - (2r^2 + l_c^2)\sqrt{(r^2 - l_c^2)}]$$

Thus

$$\bar{\sigma}_p = \frac{4\tau_y}{\pi t}\left\{l_c \sin^{-1}\sqrt{[1 - (l_c/r)^2]} + \frac{r}{3}\left(2 - \left(2 + \frac{l_c^2}{r^2}\right)\sqrt{[1 - (l_c/r)^2]}\right)\right\}.$$

If a platelet fails as soon as the stress reaches σ_{pu} anywhere in the platelet, then

$$l_c = \frac{\sigma_{pu}}{2\tau_y} t$$

and

$$\sigma_p = \frac{2\sigma_{pu}}{\pi}\left\{\sin^{-1}\sqrt{[1 - (l_c/r)^2]} + \frac{r}{3l_c}\left(2 - \left(2 + \frac{l_c^2}{r^2}\right)\sqrt{[1 - (l_c/r)^2]}\right)\right\}. \quad (13)$$

2.2. *Effects of adjacent plates*

Two symmetrical cases will be discussed. Consider first overlapping plates arranged in rows (Fig. 8a). Making the same assumptions as for the square platelets, four regions in the plate can be identified. Near the edge the stress increases from zero to $\sigma_{pu}/2$ (region 2). Next is a region where stress is constant at $\sigma_{pu}/2$ (region 4); then, as a result of adjacent platelets unloading there will be a region where the stress increases from $\sigma_{pu}/2$ to σ_{pu}, (region 3) and finally a region of constant stress, σ_{pu} (region 5).

Consider one quadrant of the platelet. Regions 2 and 3 combined are identical to regions 2 and 3 from the case where there were no adjacent plates. Region 4 has half the area included by two intersecting circles with centres separated by $r + l_c$, i.e.

$$A_4 = r^2 \sin^{-1} h/r - \frac{h}{2}(r + l_c)$$

where $h = \frac{1}{2}\sqrt{[(r - l_c)(3r + l_c)]}$, and since region 5 has area

$$A_5 = \tfrac{1}{4}\pi r^2 - (A_2 + A_3 + A_4)$$

the average stress is given by the equation

$$\bar{\sigma}_p = \frac{2\sigma_{pu}}{\pi}\left\{\sin^{-1}\sqrt{\left(1-\frac{l_c^2}{r^2}\right)} + \frac{r}{3l_c}\left(2-\left(2+\frac{l_c^2}{r^2}\right)\sqrt{\left[1-\left(\frac{l_c}{r}\right)^2\right]}\right) - \theta + \tfrac{1}{2}\left(1+\frac{l_c}{r}\right)\sin\theta\right\} \quad (14)$$

$$\text{where } \sin\theta = h/r \quad (15)$$

$\alpha = \bar{\sigma}_p/\sigma_{pu}$ and is plotted in Fig 8.

Now consider overlapping plates packed symmetrically in an equivalent fashion to close packed hexagonal. As before, there will be regions where the stress increases from 0 to $\sigma_{pu}/2$, regions where the stress is constant at $\sigma_{pu}/2$, regions where it increases to σ_{pu}, due to the unloading of plates in adjacent layers, and regions where the stress is constant at σ_{pu} (Fig. 10).

As before, it may be observed that the regions of increasing stress, when added together, are exactly equivalent to regions 2 and 3 in Fig. 13. Thus the problem reduces to determining the area where the stress is constant at $\sigma_{pu}/2$. This region contains two areas having a similar shape to area A_4, with total area

$$4r^2\phi - 2r^2\sqrt{\left[\left(1+\frac{l_c}{r}\right)^2+\frac{1}{3}\right]}\sin\phi$$

where

$$\sin\phi = \sqrt{\left[\frac{11}{12}-\frac{1}{4}\left(1+\frac{l_c}{r}\right)^2\right]} \quad (16)$$

and a region with area

$$2r^2\left(\beta - \frac{\sqrt{2}}{3} + \frac{l_c}{r}\left\{\frac{1}{\sqrt{3}} - \frac{1}{2}\sqrt{\left[1-\left(\frac{l_c}{2r}\right)^2\right]}\right\}\right)$$

where

$$\sin\beta = \sqrt{\left[\frac{2}{3}\left(1-\left(\frac{l_c}{2r}\right)^2\right)\right]} - \frac{l}{2\sqrt{3}r} \quad (17)$$

so that the total area at a constant stress of $\sigma_{pu}/2$ is

$$A_6 = 4r^2\phi - 2r^2\sqrt{\left[\left(1+\frac{l_c}{r}\right)^2+\frac{1}{3}\right]}\sin\phi + 2r^2\left(\beta - \frac{\sqrt{2}}{3} + \frac{l_c}{r}\left\{\frac{1}{\sqrt{3}} - \frac{1}{2}\sqrt{\left[1-\left(\frac{l_c}{2r}\right)^2\right]}\right\}\right). \quad (18)$$

Using the same reasoning as before, we find

$$\bar{\sigma}_p = \frac{2\sigma_{pu}}{\pi}\left\{\sin^{-1}\sqrt{\left[1-\left(\frac{l_c}{r}\right)^2\right]} + \frac{r}{3l_c}\left(2-\left(2+\frac{l_c^2}{r^2}\right)\sqrt{\left[1-\left(\frac{l_c}{r}\right)^2\right]}\right) - \frac{A_6}{4r^2}\right\}. \quad (19)$$

Again $\alpha = \bar{\sigma}_p/\sigma_{pu}$ and is plotted in Fig. 9. It will be seen that the different packing arrangements make little difference to α; for infinite aspect ratio α has the value 0.61 for the linear arrangement, and 0.56 for the hexagonal arrangement.

References

1. L. P. SUFFREDINI, AD 266-379 (1961).
2. C. F. ZAPF, *et al*, AFM2-TR-65-282 (1965).
3. L. WOHRER, A. WOSILAIT, Y. JONG, and J. ECONOMY, Paper 5-3, Fifth St. Louis Symposium on Advanced Composites (1971).
4. J. LUSIS, R. T. WOODHAMS, and M. XANTHOS, *Polymer Eng. Sci.* **13** (1973) 139.
5. G. E. PADAWER and N. BEECHER, *ibid* **10** (1970) 185.
6. M. R. PIGGOTT, *Acta Metallurgica* **14** (1966) 1429.
7. A. KELLY, "Strong Solids", (Clarendon Press. Oxford, 1966) p. 159 *et seq.*
8. V. R. RILEY, *J. Comp. Materials* **2** (1968) 436.
9. M. R. PIGGOTT, submitted to *J. Mater. Sci.* (1973).
10. *Idem J. Mech. Phys. Solids* (1973).
11. *Idem*, private communication to Fiberglas of Canada (1970).

Received 13 February and accepted 2 May 1973.